Influence of Protonation on Internal Rotation of Dimethyl Ether

Vojislava Pophristic and Lionel Goodman*

Wright and Rieman Chemistry Laboratories, Rutgers, The State University of New Jersey, New Brunswick, New Jersey 08854

Received: December 10, 1999

A model is proposed for the influence of protonation on ether potential surfaces. The model invokes the quantum-mechanical effect of protonation on the oxygen lone pair and its consequence on the internal rotation barriers and associated torsional rotation energy levels. The barrier reduction and lowered torsional energy gaps lead to possible conformational changes at ambient temperatures. The model is applied to dimethyl ether. In this case, the torsional fundamental energies become comparable to, or below, the room-temperature Boltzmann energy (depending on the proton position relative to the dimethyl ether lone pair), so that the geometry distribution in the protonated species is driven toward the asymmetric staggered−eclipsed conformer, rather than the highly preferred symmetric (C_{2v}) eclipsed−eclipsed conformer in dimethyl ether.

1. Introduction

Although potential surfaces are normally obtained via gas-phase ab initio calculations, the standard approach is to directly transfer the gas-phase potential parameters into aqueous solutions, neglecting the influence that the binding of water molecules to the solute has on the solute potential surface. Thus, the structure, barriers to internal motions, and consequently "floppiness" of molecules placed into solutions may be poorly described, especially in the case of molecules having centers suitable for either hydrogen bonding or protonation. Ether-like units, present in a number of biologically and industrially important molecules which function in aqueous solutions, provide an example of torsion around a C−O linkage susceptible to influence by protonation. There are a number of cases for which conformational preference depends on rotation around the C−O bond and, thus, on the corresponding torsional potential surface (e.g., dimethoxy methane,[1] 1,2 dimethoxyethane,[2,3] diglyme,[4] perfluorodimethoxymethane,[5] and isoflurane[6]). Moreover, gas-phase internal rotation parameters of small prototype molecules, such as methanol, dimethyl ether, dimethyl phosphate, and ethane, are often used to calibrate molecular-modeling programs for applications to larger molecules in solutions.[7,8]

We are provoked by a model earlier proposed for dimethyl ether (DME)[9] internal rotation that brings out the role of the oxygen σ lone pair orbital in the barrier energetics.[10−13] Because this is a probable center for H_2O or H^+ binding, the logical choice for examining the influence of protonation on a potential surface is DME. It is the simplest double-rotor molecule that exhibits rotation around the C−O bond, and its gas-phase potential surface has been thoroughly examined.[14−17] Our previous work[10] shows that there is a large reduction in the barrier height of dimethyl ether upon geometrically "restricted" protonation for the case in which the proton is forced to stay in the plane of the molecule. The barrier is reduced from ∼5 kcal/mol to only ∼1 kcal/mol.

In this paper, we show that protonation significantly alters the DME structure, the torsional potential surface, and the torsional frequencies. Thus, binding of protons to lone pairs in aqueous or acidic solutions should be explicitly included when dealing with conformational preferences that relate to rotation around the C−O bond.

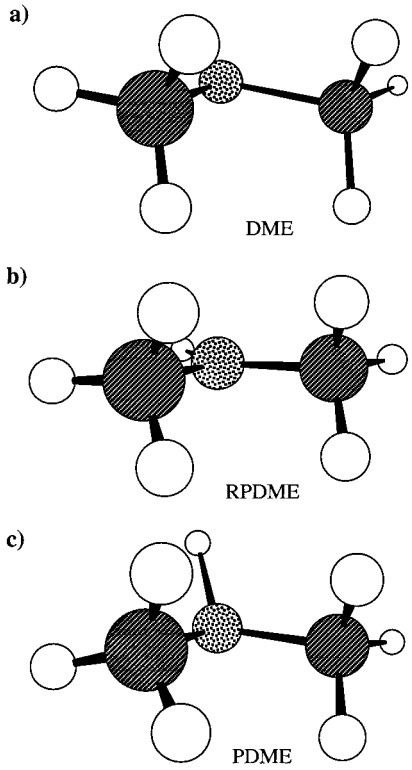

Figure 1. (a) Dimethyl ether (DME), (b) restricted protonated dimethyl ether (RPDME) and (c) fully optimized protonated dimethyl ether (PDME) equilibrium conformers. A perspective is chosen to reveal the in-plane proton in RPDME.

2. Methodology

Two forms of protonated dimethyl ether were investigated (Figure 1). The fully optimized protonated dimethyl ether (PDME) constrains only the dihedral angles that determine the relative positions of the methyl groups. Restricted protonated DME (RPDME) has an additional limitation: the OH^+ bond is confined to the COC plane throughout the rotation (but the OH^+

10.1021/jp994359p CCC: $19.00
Published on Web 03/18/2000

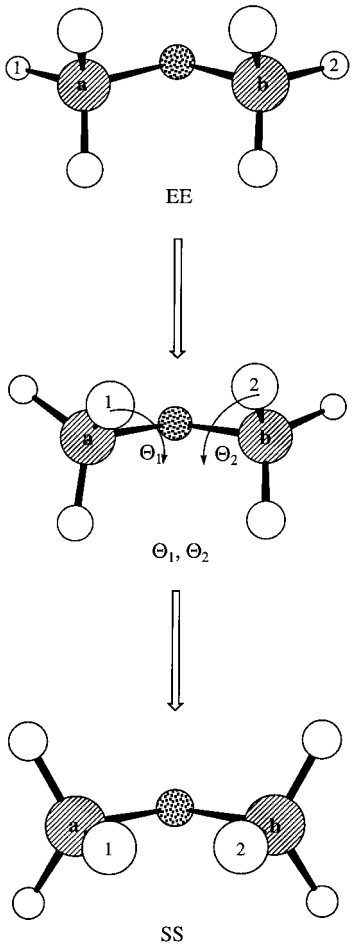

Figure 2. Dimethyl ether gearing internal rotation. The same process in RPDME and PDME involves identical motions.

bond length and COH^+ angles are not constrained). The internal rotation to the conformer, denoted as Θ_1, Θ_2, is defined as a rotation of methyl groups *a* and *b* by Θ_1 and Θ_2 angles from the ("eclipsed, eclipsed", EE) equilibrium position, respectively (Figure 2). In a double-rotor system, such as DME, we differentiate between two barriers: the rotation of a single methyl group by 180° gives the lower barrier ("staggered, eclipsed", SE, effective barrier, ΔV_{eff}), and the simultaneous 180° rotation of both methyl groups gives the upper barrier ("eclipsed, eclipsed", EE, $\Delta V_{\text{barrier}}$). These rotations, followed by full optimization, will be termed fully relaxed, or FR, rotations.

In addition, rigid-rotation (RR) analyses were performed for both of the protonated forms and DME. The point of the rigid-rotation calculation, at which all of the internal coordinates except the torsional angles are frozen at their equilibrium values, is to ascertain the impact of flexing on the potential surface. The effect of the relaxation of a particular internal coordinate on the barrier height and shape was assessed by carrying out partially relaxed rotations. In these calculations, a bond or a bond angle, or a combination of the two, was allowed to relax (i.e., assume its top-of-barrier value), whereas all of the other coordinates were kept at their equilibrium values.

The barrier heights in all cases were computed for both simultaneous ($\Delta V_{\text{barrier}}$) and single methyl group (ΔV_{eff}) rotations at various Hartree−Fock (HF) and Moller−Plesset second-order perturbation theory (MP2) levels. Both the geometry and the energy convergence are observed at the MP2/6-311G(3df,2p) level, which is then used throughout (Table 1). The results are referenced to DME itself, because our goal is to study the influence of protonation. The DME barrier height is in good agreement with Ozkabak and Goodman's[14] 1991 study and the more recent, MP2 results of Senent, Moule, and Smeyers.[16]

TABLE 1: Basis Set Effect on MP2 Barrier Heights for Synchronous ($\Delta V_{\text{barrier}}$) and Single Methyl ($\Delta V_{\text{eff}}$) Rotations (kcal/mol)[a,b]

	DME		RPDME		PDME	
basis set	$\Delta V_{\text{barrier}}$	ΔV_{eff}	$\Delta V_{\text{barrier}}$	ΔV_{eff}	$\Delta V_{\text{barrier}}$	ΔV_{eff}
6-31G(d,p)	5.06	2.81	1.03	0.46	3.69	1.75
6-31G(2d,p)	5.20	2.86	1.23	0.56	4.06	1.86
6-31G(3df,2p)	4.72	2.60	1.14	0.50	3.80	1.76
6-311G(3df,2p)	4.72	2.62	1.24	0.58	3.62	1.72
6-311++G(3df,2p)	4.77	2.64	1.29	0.59	3.60	1.68

[a] Geometry optimizations are carried out at the indicated MP2 level. [b] Values are rounded off to the nearest 0.01 kcal/mol.

TABLE 2: Potential Energy Constants (kcal/mol) and Torsional Fundamental frequencies (cm^{-1})[a]

	DME	RPDME	PDME
	potential constants[b]		
V_3	2.37	0.62	1.81
V_{33}	−0.25	0.04	0.09
V'_{33}	0.08	−0.06	−0.10
V_6	0.01	0.03	0.04
	fundamental frequencies		
gearing	232	107	186
antigearing	199	82	148

[a] Potential constants are obtained by fitting eq 1 from MP2/6-311G(3df,2p) energies of nine MP2/6-311G(3df,2p) optimized conformers. [b] See footnote *b*, Table 1.

The potential surface for all three cases was constructed from a set of nine optimized conformers. Potential constants were derived from a four-term Fourier expansion for double-rotor systems appropriate to C_{3v} methyl groups:

$$\Delta V(\Theta_1,\Theta_2) = \frac{1}{2}V_3(\cos 3\Theta_1 + \cos 3\Theta_2) + \frac{1}{2}V_{33}\cos 3\Theta_1 \cos 3\Theta_2 + \frac{1}{2}V'_{33}\sin 3\Theta_1 \sin 3\Theta_2 + \frac{1}{2}V_6(\cos 6\Theta_1 + \cos 6\Theta_2) \quad (1)$$

where Θ_1 and Θ_2 are torsional angles of the two methyl groups[18] (Figure 2), and $\Delta V(\Theta_1,\Theta_2)$ is the energy of the Θ_1, Θ_2 conformer relative to the equilibrium one. The four V_i constants determine barrier height (V_3) and barrier shape (V_{33},V'_{33},V_6). In general, a set of four V_i constants can be obtained from the energies of five conformers (the equilibrium energy is used to fix the constant term in the Fourier expansion). However, to improve the reliability of the resulting surface, a set of nine conformers was used.[19] The root-mean-square error of the nine conformer energies with respect to eq 1 is ≤ 0.01 kcal/mol in all three cases. The V_i constants are given in Table 2. In terms of these constants, the effective and simultaneous rotation barriers can be represented as $\Delta V_{\text{eff}} = V_3 - V_{33}$ and $\Delta V_{\text{barrier}} = 2V_3$.

Equation 1 holds for molecules with 3-fold potentials, i.e., for rotors having C_{3v} symmetry. The symmetry condition is not strictly valid (i.e., the HCH angles and C−H bond lengths are unequal, Table 3) for all three species. However, a simulation of the experimental torsional gearing frequency is good for the worst offender, DME, when eq 1 is used.[14,15] Both of the protonated cases show 3-fold potentials and fulfill the C_{3v} methyl group requirement more closely than DME (i.e., there is less disparity in the HCH angles and C−H bond lengths), providing further justification for using eq 1. The gearing fundamental

TABLE 3. MP2/6-311G(3df,2p) Optimized Geometries of Equilibrium (EE) and Top-of-Barrier (SS) Conformers

	DME		RPDME		PDME	
	EE	SS	EE	SS	EE	SS
bond length (Å)						
C−O	1.405	1.409	1.468	1.475	1.480	1.485
C−H_{ip}	1.086	1.092	1.083	1.082	1.083	1.082
C−H^1_{op}[a]	1.095	1.091	1.084	1.083	1.085	1.083
C−H^2_{op}[a]					1.083	1.082
O−H			0.964	0.966	0.971	0.967
distance (Å)						
C−H_{ip}/C−H_{ip}	4.028	2.033	4.108	2.196	4.117	2.130
C−H_{op}/C−H_{op}[b]	2.413	3.573	2.629	3.662	2.533	3.627
C−H_{op}/C−H_{op}[c]					2.470	3.663
C−H_{op}/C−H_{op}[d]	2.997	3.988	3.188	4.082	3.082	4.066
bond angle (deg)						
COC	111.3	116.9	121.9	125.9	115.8	121.9
H_{ip}CO	107.5	111.9	106.3	105.6	105.9	106.6
H^1_{op}CO[a]	111.4	109.8	107.1	107.4	108.8	107.6
H^2_{op}CO[a]					105.2	106.3
COH			119.0	119.1	111.2	113.0
dihedral angle (deg)						
COHC			180.0	180.0	128.2	139.9

[a] Indexes 1 and 2 refer to hydrogen atoms on the same and opposite side of the COC plane as the tilted OH^+ bond, respectively. [b] Corresponds to the distance between two out-of-plane hydrogen atoms of different methyl groups, located on the same side of the COC plane (in case of PDME, also on the same side as the tilted OH^+ bond in the EE conformer). [c] Corresponds to the distance between two out-of-plane hydrogen atoms of different methyl groups, both located on the same side of the COC plane, opposite of the tilted OH^+ bond in the EE conformer. [d] Corresponds to the distance between two out-of-plane hydrogen atoms of different methyl groups, located on the opposite sides of the COC plane.

experimental frequency for DME has been reported,[20] but no experimental or theoretical work on the protonated species' potential surface or frequencies is available. Our goal is to obtain potential surfaces and predict the trends in torsional frequencies caused by protonation. There are two reasons to focus on frequencies: first, these are observables that relate to potential surfaces, and second, the torsional energy levels control Boltzmann factors relating to conformational changes.

The computations were performed using Gaussian 94[21a] and Gaussian 98[21b] software. They were carried out on a Cray T90 at the San Diego Supercomputer Center and on SGI Origin 200 and Dual Pentium Pro 200 computers at Rutgers University. The torsional frequencies were calculated using TACIR.[21c]

3. Torsional Potential Surfaces

A. Dimethyl Ether (DME). The optimized dimethyl ether equilibrium conformer (Figure 1a) has C_{2v} symmetry at all of the calculation levels attempted. The two in-plane hydrogens (C−H_{ip}) are trans with respect to the C−O bonds, eclipsing the oxygen atom ("eclipsed, eclipsed", EE conformer). Methyl groups depart significantly from local C_{3v} symmetry because of the nearly 4° disparity between the H_{ip}CO and the H_{op}CO angles (Table 3). The metastable (SS, Figure 2) conformer is reached by the simultaneous rotation of both methyl groups by 180°, preserving the equilibrium C_{2v} symmetry with nearly C_{3v} methyl tops; in-plane hydrogens are now cis to the C−O bonds. The most noticeable geometrical change during the EE → SS process is COC angle opening. As discussed in our previous studies,[10−13] this flexing is caused by the increased repulsion between methyl groups during rotation. The importance of this relaxation was first noted in early studies by Ha et al.[17] Ozkabak and Goodman[14] showed that the fully relaxed potential surface (including the COC angle opening) gives the gearing frequency

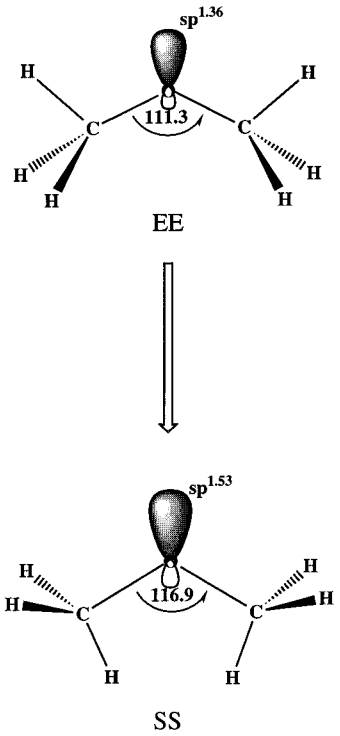

Figure 3. Schematic depiction of oxygen σ lone pair orbital reorganization accompanying internal rotation in dimethyl ether (DME).

TABLE 4. Barrier Relaxation Effects (kcal/mol)[a,b,c]

	DME	RPDME	PDME
RR[d]	7.23	1.69	5.13
OH^+ tilt angle			5.34
CO bond length	7.10	1.64	5.06
CH_3 group flexing	5.91	1.65	4.50
COC angle	5.79	1.39	4.72
COC angle & CH_3 group flexing	4.74	1.35	4.15
FR[e]	4.72	1.24	3.62

[a] Simultaneous rotation of both methyl groups plus indicated relaxation. [b] See footnote *b*, Table 1. [c] MP2/6-311G(3df,2p) energy calculation, based on MP2/6-311G(3df,2p) optimized geometries. [d] Rigid rotation, RR, all coordinates frozen except torsional angles. [e] Fully relaxed rotation, FR, all coordinates optimized, except torsional angles.

in good agreement with IR measurements. Moule and coworkers[16] subsequently showed that a three-dimensional hypersurface, with respect to the COC angle and the torsional angles of the methyl groups, gives a still better account of the spectroscopic details than the fully relaxed surface. Additionally, our studies[10,13] indicate that the physics of the barrier cannot be correctly appreciated if flexing is not present as a part of the mechanism.

We focus on the synchronous rotation of both methyl groups to obtain the potential curves that correspond to gearing (methyl groups rotate in opposite directions) and antigearing modes (methyl groups rotate in the same direction). The ab initio computed DME barrier for this process is unusually high for bimethyl rotors (4.7 kcal/mol). For example, it is much higher than in acetone (∼2.3 kcal/mol).[22] On the basis of energy partitioning[10] developed in a natural bond orbital (NBO) formalism,[23] we found that the reason for such a high barrier energy lies in the prominent role played by the oxygen σ lone pair in the barrier energetics. During synchronous rotation, two C−H_{ip} bonds come close to each other, and they repel each other. The response to the increased strain is COC angle

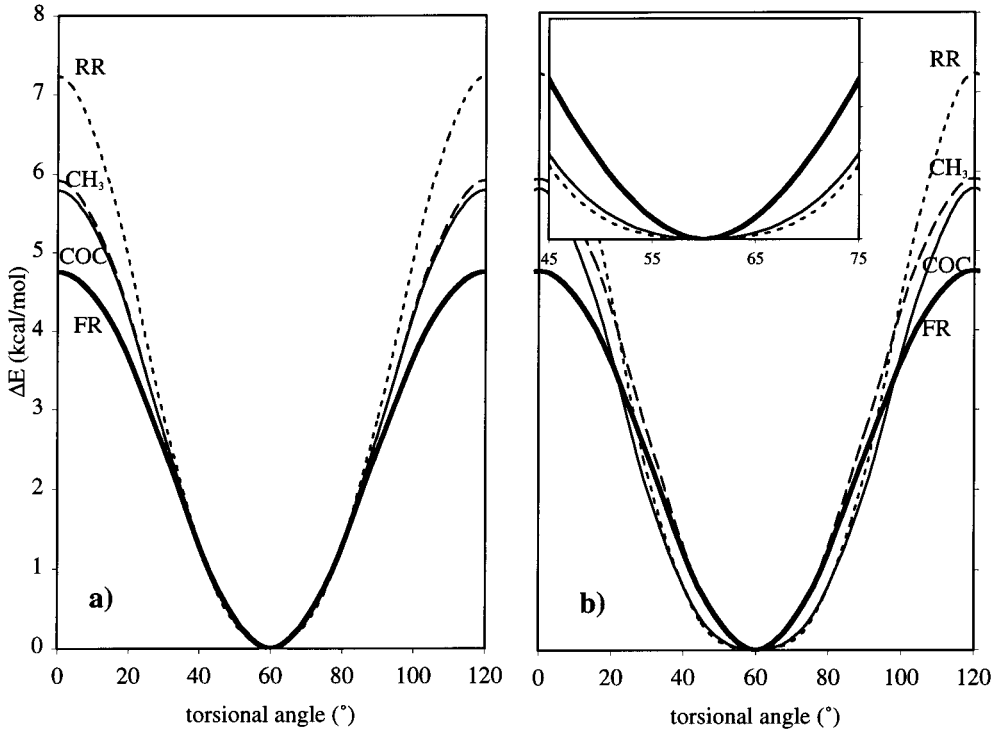

Figure 4. Dimethyl ether (DME) antigearing (a) and gearing (b) torsional potential wells for fully relaxed, rigid, and (two) partially relaxed rotations. Inset focuses on the low-energy region of the gearing well. Fully relaxed rotation, full bold line; rigid rotation, dotted line; COC angle opening plus rotation, full line; CH_3 group folding plus rotation, dashed line.

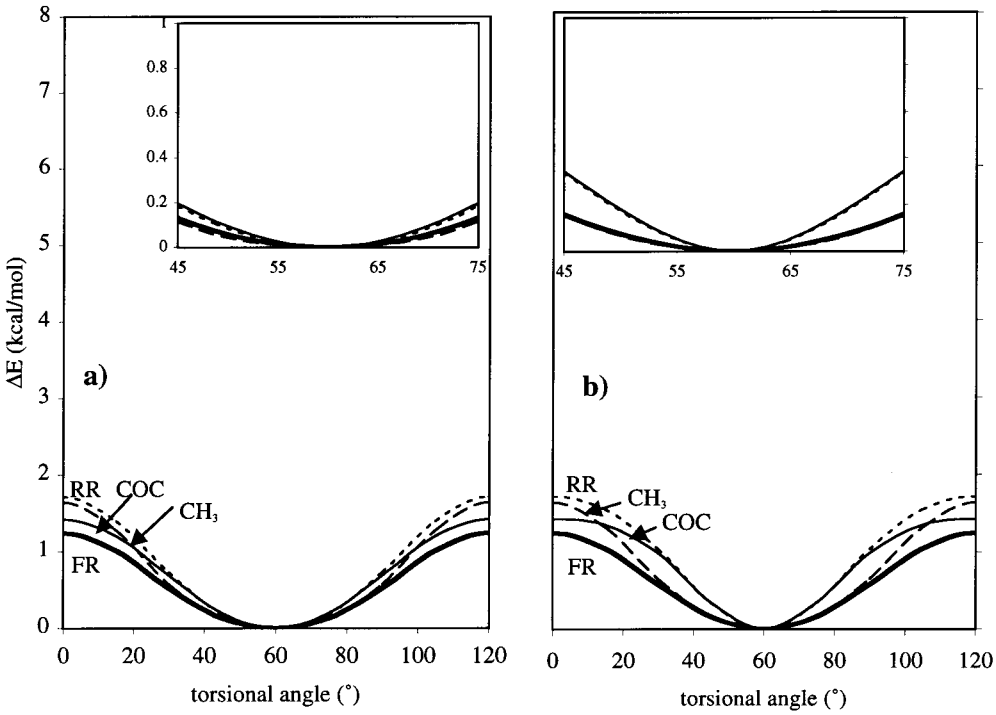

Figure 5. Restricted protonated dimethyl ether (RPDME) antigearing (a) and gearing (b) torsional potential wells for fully relaxed, rigid, and (two) partially relaxed rotations. Insets focus on the low-energy regions of the corresponding wells. Line denotation same as in Figure 4.

opening, which in turn triggers reorganization of the oxygen σ lone pair orbital (Figure 3). Its hybridization[24] changes from $sp^{1.36}$ to $sp^{1.53}$. (In effect, the p character is enhanced as a consequence of the increased interaction between the C−O bonds and the σ lone pair.) The energy change of this orbital is the largest barrier-forming energy term in DME. The lack of an equivalently placed σ lone pair in acetone rationalizes the much lower barrier in this molecule.

The effect of relaxation is broken down in Table 4. Because of its triggering role, it is to be expected that the opening of the COC angle significantly influences barrier height and shape. The RR barrier is ∼2.5 kcal/mol higher than the FR barrier (4.7 kcal/mol, Table 4). Allowing COC angle relaxation reduces the RR barrier by ∼20%, to ∼5.8 kcal/mol. A significant effect (−1.3 kcal/mol) is also observed for CH_3-group relaxation, due to the interaction between the methyl groups. An important outcome is that both of these relaxations are required to simulate the fully relaxed barrier energy.

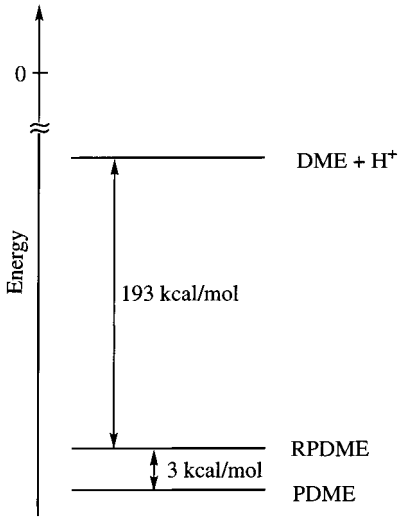

Figure 6. Positions of DME, PDME, and RPDME equilibrium conformers on the energy scale.

The impact of relaxation on the barrier shape is more complex and must be considered separately for gearing and antigearing modes (Figure 4). In analyzing the potential wells, we put emphasis on their form in the low-energy region, which determines the torsional fundamental energies. The gearing potential curve strongly depends on the relaxation details. The contrast between the factors affecting barrier height and shape is illustrated by the roles of the COC angle opening and the methyl group flexing. The angle widening is the most important relaxation in interpreting barrier height, but it is the methyl group flexing that is the determinant for the low-energy region of the gearing-potential curve. In contrast to the strong relaxation sensitivity found for the gearing potential, the antigearing torsional potential curve is insensitive to molecular relaxation.

We report the gearing and antigearing frequencies calculated from the MP2/6-311G(3df,2p) potential surface (Table 2). The 232 cm^{-1} gearing fundamental is in qualitative agreement with the experimentally determined value of 241 cm^{-1}.[20] The yet unmeasured antigearing frequency is predicted at 199 cm^{-1}. Noteworthy is the relatively small (33 cm^{-1}) separation between gearing and antigearing fundamental frequencies. The analogous difference in acetone is 48 cm^{-1}, despite the lesser steric contact between methyl rotors.

B. Restricted Protonated Dimethyl Ether (RPDME). A question that naturally arises from the DME internal rotation mechanism[10] is the following: what happens if the rehybridization of the σ lone pair orbital is blocked? Such blocking can be achieved by protonating the oxygen σ lone pair, constraining the OH^+ bond to the COC plane (restricted protonated dimethyl ether, RPDME, Figure 1b). As this rehybridization mechanism predicts, RPDME exhibits a very low barrier (1.2 kcal/mol). The torsion around the C−O bond becomes much freer, making the potential surface strongly flattened.

RPDME has the same (EE) conformational preference as DME, retaining DME's C_{2v} symmetry at both the bottom and the top of the barrier (Figure 1b). However, it has longer C−O bonds and a larger COC angle (Table 3), thus weakening the interaction between methyl groups. There is another important difference: the methyl groups are closer in shape to C_{3v}-symmetry rotors, as seen from the reduced disparity between $H_{ip}CO$ and $H_{op}CO$ angles and $C-H_{ip}$ and $C-H_{op}$ bond lengths. The OH^+ bond replaces the important barrier contributing oxygen σ lone pair orbital in DME. This, along with the lowered methyl−methyl interaction, reduces the barrier to only 1.2 kcal/mol.

The COC angle opening and CH_3 group flexing still play important roles in determining barrier height and shape (Figure 5), with the COC angle opening as the most important relaxation influencing the barrier height (Table 4). Analogous to DME, relaxations accompanying torsion do not strongly affect the form

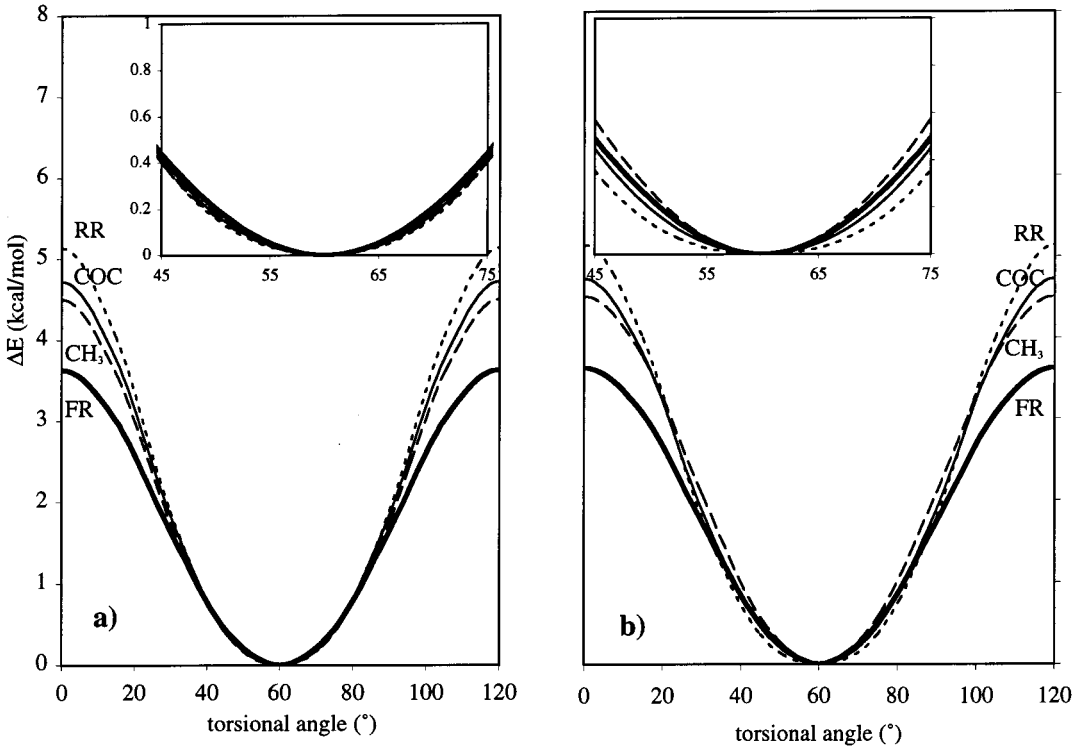

Figure 7. Protonated dimethyl ether (PDME) antigearing (a) and gearing (b) torsional potential wells for fully relaxed, rigid, and (two) partially relaxed rotations. Insets focus on the low-energy regions of the corresponding wells. Line denotation same as in Figure 4.

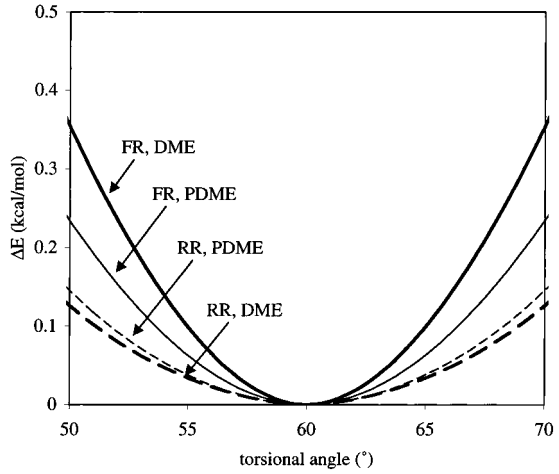

Figure 8. Low-energy region of the gearing mode potential wells for DME and PDME. Rigid rotation, dashed lines; fully relaxed rotation, full lines.

of the antigearing potential, but their influence is evident for the gearing potential (Figure 5). The shape of both potentials is well simulated by CH_3 flexing alone. However, the combination of these two flexings is required to approximate the full FR (i.e., both barrier height and shape) behavior (Table 4 and Figure 5).

The changes in the curvature of the potential surfaces have important implications for both gearing and antigearing fundamental frequencies. (It is the V_{33} constant that changes dramatically between DME and RPDME, Table 2.) The predicted frequencies are reduced by $\sim$100 cm^{-1}, and from a bioenergetic viewpoint, the available energy at room temperature, kT_R, is well above both gearing and antigearing fundamental and overtone energies (Table 2).

C. Protonated Dimethyl Ether (PDME). The effect of the constrained protonation of the σ lone pair is a large reduction in the barrier height. However, we find that such protonation is not the most energetically favorable one (Figure 6).[25] In free, unrestricted oxygen protonation (PDME), the symmetry of the optimized geometry for all of the calculation levels employed is reduced to C_s in both conformers because of the OH^+ bond $\sim$50° tilt out of the COC plane (Table 3). Upon torsion, the tilt angle is reduced by 11.7°. The equilibrium COC angle is 4.5° wider than in DME, and during torsion, it opens by an additional 6°. The C−O bonds are also longer than in DME. Thus, the two methyl groups are significantly more separated than in DME but not as much as in RPDME. Note that the EE conformational preference does not change for PDME.

The effect of unrestricted protonation is to still reduce the barrier but less so than in RPDME. The 3.6 kcal/mol barrier is affected by the same flexings that are important in DME itself. The OH^+ bond flexing continues to be unimportant. The general trend of relaxation effects on the barrier shape follows the DME pattern as well: the antigearing potential remains insensitive to relaxation, whereas combined CH_3 folding and COC angle opening simulate the FR curvature of the gearing potential (Figure 7). However, there is an important difference between DME and PDME: in the low energy region, the PDME well is wider than the DME one, inducing much lower torsional fundamental frequencies (antigearing, 148 cm^{-1}; gearing, 186 cm^{-1}). Although the order of importance of various flexings on the barrier curvature is the same in DME and PDME, the actual impact is very different. As can be seen in Figure 8, the shapes of the DME RR and FR curves are less congruent than in PDME, leading to the conclusion that the influence of relaxation in PDME is reduced from DME. Both the wider and the shallower well (and, consequently, lower torsional frequencies) and the decreased flexing impact can be understood as consequences of the increased distance between CH_3 groups. The larger COC angle, even though its change is similar to that in DME, explains both the weaker COC angle opening-torsion couplings and the weaker methyl folding-torsion couplings, causing lower overall relaxation influence on the barrier shape.

TABLE 5. Symmetry Decomposition of Nuclear−electron Attraction Energy Changes (kcal/mol)[a]

	DME	RPDME		PDME
nuclear−electron attraction (ΔE_{ne})	766	505		732
$A_1(\sigma)$	318	173		
$A_2(\pi)$	252	199	A'^b	378
$B_1(\pi)$	109	119	A''^c	354
$B_2(\sigma)$	88	15		

[a] Rounded off to the nearest 1 kcal/mol. [b] A' contribution in PDME (C_s symmetry) corresponds to the sum of $A_1(\sigma)$ and $B_1(\pi)$ symmetry terms in C_{2v} molecules. [c] A'' contribution in PDME (C_s symmetry) corresponds to the sum of $A_2(\pi)$ and $B_2(\sigma)$ symmetry terms in C_{2v} molecules.

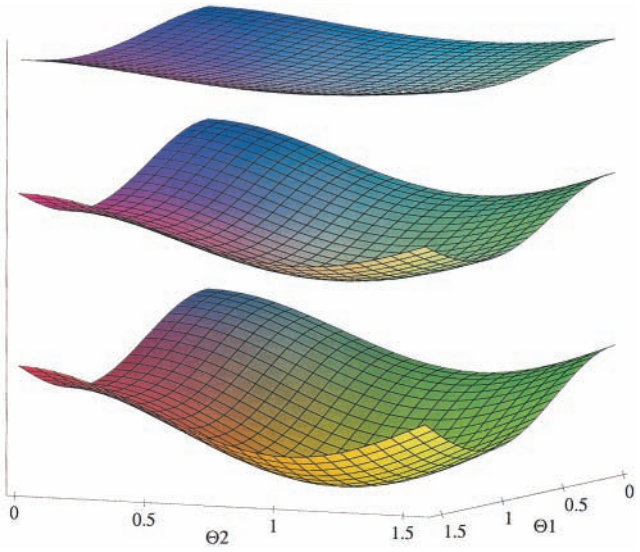

Figure 9. Torsional potential surfaces for DME (bottom), PDME (middle), and RPDME (top). Their relative position on the energy scale (identical for all three surfaces) is arbitrary.

4. Discussion

The extent to which protonation influences the molecular geometry correlates with its effect on the potential surface. The most prominent geometrical effects involve the COC angle and the CO bond length, increasing in the order DME < PDME < RPDME and making the methyl groups further apart in the same sense. Consequently, the COC angle bending−methyl torsion coupling, major in DME, is attenuated in PDME and RPDME. The same geometrical alterations are responsible for the decreased methyl top-methyl top interactions. The V_{33} potential constant that determines the average coupling,[26] and consequently, the average torsional fundamental energy, is significantly reduced upon protonation, becoming almost negligible in RPDME.

Some insight into the electronic interactions that influence the barrier can be obtained by considering the nuclear−electron attraction (ΔE_{ne}), electron−electron and nuclear−nuclear repulsion and kinetic energy changes. We have already shown that only the ΔE_{ne} term is barrier forming for several related

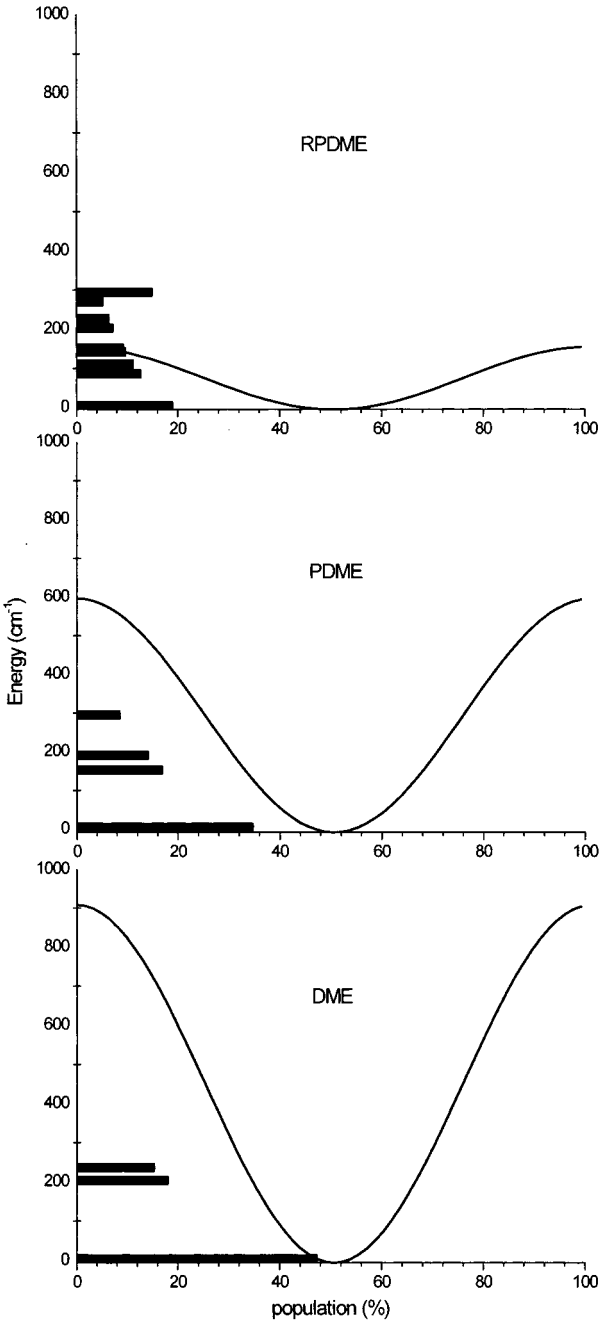

Figure 10. Room-temperature Boltzmann populations of the low-lying torsional levels ($\leq$300 cm^{-1} above the torsional zero-point energy) for protonated species and DME. Also shown are potential curves for single methyl group rotation from the SE to the SE conformer (minimum is EE). Levels that are too close to be resolved are represented by a single bar.

molecules,[12] and we confirm this for all three species being discussed here (Table 5). The magnitude of ΔE_{ne} decreases in the order DME > PDME > RPDME. In C_{2v} DME and RPDME, ΔE_{ne} breaks down into $A_1(\sigma)$ (containing the oxygen σ lone pair in DME and OH^+ bond in RPDME), $A_2(\pi)$, $B_1(\pi)$ (containing classical π contributions, such as hyperconjugation and π lone-pair contributions), and $B_2(\sigma)$ categories. For C_s PDME, the components are A′ and A″. The contribution from the OH^+ bond in RPDME is reduced in comparison with the σ oxygen lone pair in DME.[10] This effect, caused by the blocking of rehybridization through protonation, is reflected by the reduced $A_1(\sigma)$ term (Table 5).

In PDME, the interactions cannot be identified as being either σ or π: $A_1(\sigma)$ and $B_1(\pi)$ categories in DME and RPDME become A′, whereas $A_2(\pi)$ and $B_2(\sigma)$ become A″. Table 5 shows that the combined $A_1(\sigma)$ and $B_1(\pi)$ ΔE_{ne} terms in DME have a larger barrier-forming character than the A′ one in PDME, which in turn is larger than the combination in RPDME, consistent with the flattening of the torsional surface. The C−O bonds change their s oxygen character in a manner consistent with the ΔE_{ne} change: in PDME, it increases during the rotation more than in DME, which lowers the barrier.

5. Conclusions

Our principal conclusion is that protonation strongly affects the DME internal rotation potential surface and structure. This influence is largely determined by the position of the proton with respect to the molecular (COC) plane. The effect is most pronounced for the case in which the proton is able to directly bind with the σ lone pair, i.e., when the OH^+ bond is in the molecular plane, as in RPDME. The dependence of the barrier height and curvature on the proton position is illustrated in Figure 9. It is also interesting to note the relative order of the DME, PDME, and RPDME surfaces on the energy scale (Figure 6), both the spacing and sequence implying that protonation of DME is an energetically favorable process.

An important consequence of protonation is the dramatic decrease in torsional vibration frequencies. The sensitivity to the proton position suggests that *torsional* frequencies can serve as a diagnostic for the position of the complexing agent relative to the molecule.

For both protonated species, the frequency lowering is large enough to significantly change the Boltzmann populations of these levels. The outcome is that upon protonation the density of low-lying torsional levels increases, with consequent population enhancement (Figure 10). A molecule, undergoing internal rotation, will pass through the asymmetric SE transition state, in which only a single methyl group has rotated, if its energy approaches ΔV_{eff}. This process is unlikely in DME because the energy gap between the significantly populated levels and ΔV_{eff} at room temperature is $\sim 3kT_R$. On the other hand, in the protonated species, the energy gap is much smaller, if existent at all. In PDME, it is only $1.5kT_R$, and RPDME undergoes practically free rotation!

This conclusion has potentially important conformational consequences. In ROR′ molecules (R, R′ being more complex rotating groups), the preferred isolated molecule conformation may undergo an important change on protonation or hydrogen bonding.

Acknowledgment. We thank Dr. Peter Groner for providing us with TACIR, used to calculate the torsional frequencies from potential surfaces. Financial support from NSF and computational support from the San Diego Supercomputer Center are gratefully acknowledged.

References and Notes

(1) Wiberg, K. B.; Murcko, M. A. *J. Am. Chem. Soc.* **1989**, *111*, 4821.
(2) Williams, D. J.; Hall, K. B. *J. Phys. Chem.* **1996**, *100*, 8224.
(3) Liu, H.; Muller-Plathe, F.; van Gunsteren, F. *J. Chem. Phys.* **1995**, *102*, 1722.
(4) Sutjianto, A.; Curtiss, L. A. *Chem. Phys. Lett.* **1997**, *264*, 127.
(5) Stanton, C. L.; Schwartz, M. *J. Phys. Chem.* **1993**, *97*, 11 221.
(6) Polavarpu, P. L.; Cholli, A. L.; Vernice, G. *J. Am. Chem. Soc.* **1992**, *114*, 10 953.
(7) Kollman, P. A. *Acc. Chem. Res.* **1996**, *29*, 461.
(8) Cornell, W. D.; Cieplak, P.; Bayly, C. I.; Gould, I. R.; Merz, K. M., Jr.; Ferguson, D. M.; Spellmeyer, D. C.; Fox, T.; Caldwell, J. W.; Kollman, P. A. *J. Am. Chem. Soc.* **1995**, *117*, 5179.

(9) Not to be confused with 1,2-dimethoxy ethane, which is often abbreviated in the same way.

(10) Pophristic, V.; Goodman, L.; Guchhait, N. *J. Phys. Chem.* **1997**, *101*, 4290.

(11) Goodman, L.; Pophristic, V. *Chem. Phys. Lett.* **1996**, *259*, 287.

(12) Goodman, L.; Pophristic, V. Rotational Barriers: Barrier Origins. In *The Encyclopedia of Computational Chemistry*; Schleyer, P. v. R., Allinger, N. L., Clark, T., Gasteiger, J., Kollman, P. A., Schaefer, H. F., III, Schreiner, P. R., Eds.; John Wiley & Sons: Chichester, 1998; Vol. 4; pp 2525−2541.

(13) Goodman, L.; Pophristic, V.; Weinhold, F. *Acc. Chem. Res.* **1999**, *32*, 983.

(14) Ozkabak, A. G.; Goodman, L. *Chem. Phys. Lett.* **1991**, *176*, 19.

(15) Senent, M. L.; Moule, D. C.; Smeyers, Y. G. *Can. J. Phys.* **1995**, *73*, 425.

(16) Senent, M. L.; Moule, D. C.; Smeyers, Y. G. *J. Chem. Phys.* **1995**, *102*, 5952.

(17) Ha, T.-K.; Groner, P.; Bauder, A.; Gunthard, H. H. *Chem. Phys.* **1978**, *33*, 27.

(18) Torsional angles Θ_1 and Θ_2 are defined as angular positions of H_1C_a, H_2C_b relative to $O-C_b$, $O-C_a$, respectively (Figure 2). In-phase rotation is usually denoted as gearing, out-of-phase rotation is usually denoted as antigearing.

(19) 0, 0; 180, 180; 0, 180; 210, 210; 180, 210; 195, 195; 195, 210; 210, 240; 180, 195 conformers.

(20) Groner, P.; Durig, J. R. *J. Chem. Phys.* **1977**, *66*, 1856.

(21) (a) Frisch, M. J.; Trucks, G. H.; Schlegel, H. B.; Gill, P. M. W.; Johnson, B. J.; Robb, M. A.; Cheeseman, J. R.; Keith, T.; Petersson, G. A.; Montgomery, J. A.; Raghavachari, K.; Al-Laham, M. A.; Zakrzewski, V. G.; Ortiz, J. V.; Foresman, J. B.; Cioslowski, J.; Stefanov, B. B.; Nanayakkara, A.; Challacombe, M.; Peng, C. Y.; Ayala, P. Y.; Chen, W.; Wong, M. W.; Andres, J. L.; Replogle, E. S.; Gomperts, R.; Martin, R. L.; Fox, D. J.; Binkley, J. S.; Defrees, D. J.; Baker, J.; Stewart, J. P.; Head-Gordon, M.; Gonzalez, C.; Pople, J. A. Gaussian 94; Gaussian, Inc.: Pittsburgh, PA, 1995. (b) Fisch, M. J.; Trucks, G. H.; Schlegel, H. B.; Scuseria, G. E.; Robb, M. A.; Cheeseman, J. R.; Zakrzewski, V. G.; Montgomery, J. A.; Stratmann, R. E.; Burant, J. C.; Dapprich, S.; Millam, J. M.; Daniels, A. D.; Kudin, K. N.; Strain, M. C.; Farkas, O.; Tomasi, J.; Barone, V.; Cossi, M.; Cammi, R.; Mennucci, B.; Pomelli, C.; Adamo, C.; Clifford, S.; Ochterski, J.; Petersson, G. A.; Ayala, P. Y.; Ciu, Q.; Morokuma, K.; Malick, D. K.; Rabuck, A. D.; Raghavachari, K.; Foresman, J. B.; Cioslowski, J.; Ortiz, J. V.; Stefanov, B. B.; Liu, G.; Liashenko, A.; Piskorz, P. Komaromi, I.; Gomperts, R.; Martin, R. L., Fox, D. J.; Keith, T.; Al-Laham, M. A.; Peng, C. Y.; Nanayakkara, A.; Gonzalez, C.; Challacombe, M.; Gill, P. M. W.; Johnson, B. G.; Chen, W.; Wong, M. W.; Andres, J. L.; Head-Gordon, M.; Replogle, E. S.; Pope, J. A. Gaussian 98; Gaussian, Inc.: Pittsburgy, PA, 1998. (c) Groner, P. Private communication.

(22) Ozkabak, A. G.; Philis, J. G.; Goodman, L. *J. Am. Chem. Soc.* **1990**, *112*, 7854.

(23) Weinhold, F. Natural Bond Orbital Methods. In *The Encyclopedia of Computational Chemistry*; Schleyer, P. v. R., Allinger, N. L., Clark, T., Gasteiger, J., Kollman, P. A., Schaefer, H. F., III, Schreiner, P. R., Eds.; John Wiley & Sons: Chichester, 1998; pp 1792−1811.

(24) The hybridization is somewhat basis-set dependent; our previous studies report a slightly different composition for the oxygen lone pair orbital, but the general sense of sp hybridization change is preserved.

(25) Some hydrogen-bonding species are believed to form planar complexes with DME (see: Asselin, P.; Dupuis, B.; Perchard, J. P.; Soulard, P. *Chem. Phys. Lett.* **1997**, *268*, 265. and Audier, H. E.; Koyanagi, G. K.; McMahon, T. B.; Tholmann, D. *J. Phys. Chem.* **1996**, *100*, 8220); For an example of a nonplanar complex involving DME, see: Rablen, P. R.; Lockman, J. W.; Jorgensen, W. L. *J. Phys. Chem.* **1998**, *102*, 3782.

(26) Senent, M. L.; Moule, D. C.; Smeyers, Y. G. *J. Mol. Struct.* **1995**, *372*, 257.